Neurochemistry International 126 (2019) 218–228

Contents lists available at ScienceDirect

Neurochemistry International

journal homepage: www.elsevier.com/locate/neuint

Metabotropic glutamate receptor 5 ablation accelerates age-related neurodegeneration and neuroinflammation

Toniana G. Carvalho[a], Juliana Alves-Silva[b], Jessica M. de Souza[a], Ana L.C.V. Real[a], Juliana G. Doria[a], Erica L.M. Vieira[c], Giovanni F. Gomes[d], Antonio C. de Oliveira[d], Aline S. Miranda[b], Fabiola M. Ribeiro[a,*]

[a] Department of Biochemistry and Immunology, Institute of Biological Sciences (ICB), Universidade Federal de Minas Gerais, Belo Horizonte, MG, 31270-901, Brazil
[b] Department of Morphology, Institute of Biological Sciences (ICB), Universidade Federal de Minas Gerais, Belo Horizonte, MG, 31270-901, Brazil
[c] Interdisciplinary Laboratory of Medical Investigation, School of Medicine, Universidade Federal de Minas Gerais, Belo Horizonte, MG, 30130-100, Brazil
[d] Department of Pharmacology, Institute of Biological Sciences (ICB), Universidade Federal de Minas Gerais, Belo Horizonte, MG, 31270-901, Brazil

ARTICLE INFO

Keywords:
$mGlu_5$ receptor
Aging
Neuroinflammation
Neurodegeneration
Huntington's disease

ABSTRACT

The growing elderly population world widely prompts the need for studies regarding aged brain and its susceptibility to neurodegenerative diseases. It has been shown that aged brain exhibits several alterations, including neuroinflammation, which prone this organ to neurodegenerative processes. Metabotropic glutamate receptor 5 ($mGlu_5$ receptor) has a role in neuronal cell loss and inflammation. Although the relevance of $mGlu_5$ receptor in different diseases has been investigated, its involvement in normal brain aging remains unclear. In the present study, we used the $mGlu_5$ receptor knockout ($mGluR5^{-/-}$) mice, a model of Huntington's Disease (BACHD), and the double mutant mice ($mGluR5^{-/-}$/BACHD), at the ages of 2, 6 and 12 months, to investigate whether $mGlu_5$ receptor has a role in brain aging. We demonstrated that $mGluR5^{-/-}$ mice exhibit diminished number of neurons at 12 months of age in the cortex and striatum, similarly to what was observed in the case of BACHD and $mGluR5^{-/-}$/BACHD mice. In addition, ablation of $mGlu_5$ receptor increased the number of astrocytes and microglia in BACHD and wild type (WT) mice in an age-dependent manner in the cortical region, but not in the striatum. Interestingly, 12-month-old $mGluR5^{-/-}$ mice induced microglia activation, evidenced by increased CD68 expression and diminished number of microglia ramifications in skeleton analyses. Importantly, the presence of mutant huntingtin and the absence of $mGlu_5$ receptor promoted decreased levels of fractalkine expression in aged mice, which could account for the decreased levels of microglia activation in these mice. Together, our data provide evidence that $mGlu_5$ receptor plays a role in brain aging by modulating different cell types in the central nervous system (CNS).

1. Introduction

The global population aged 60 years or over was estimated at 962 million in 2017, much more than in 1980 when the number of elderly was around 382 million, according to the Department of Economic and Social Affairs of United Nation. In 2030, elderly people are expected to outnumber children under the age of 10 (1.41 billion versus 1.35 billion). This demographic transition, which is occurring throughout the world, results from the decline in fertility and improvement in survival (United Nations, 2017). One of the main issues afflicting this population aged 60 years or over is the high prevalence of neurodegenerative diseases, which accelerates brain shortfalls in an age-dependent manner. Therefore, more studies are necessary to understand brain aging and its susceptibility to neurodegenerative diseases.

Post-mortem studies have shown that aged brains display numerous degenerative features, such as atrophy, protein deposition and several

Abbreviations: BDNF, brain derived neurotrophic factor; CREB, cAMP responsive element binding protein; CNS, Central nervous system; CBP, CREB binding protein; CX3CL1, (C-X3-C motif) ligand 1; CX3CR1, (C-X3-C Motif) Receptor; HD, Huntington's Disease; htt, huntingtin; IL1-β, Interleukin 1 beta; InsP3, inositol-1,4,5-triphosphate; MCP-1, monocyte chemotactic protein 1; mGlu receptor, metabotropic glutamate receptor; NeuN, neuronal marker; NF-κB, Factor nuclear kappa B; PLC, phospholipase Cβ1; TGF-β3, transforming growth factor beta 3; TNF-α, tumor necrosis factor-α

* Corresponding author. Department of Biochemistry and Immunology, Institute of Biological Sciences (ICB), Universidade Federal de Minas Gerais, Ave. Antonio Carlos 6627, Belo Horizonte, MG, CEP: 31270-901, Brazil.
E-mail address: fmribeiro@icb.ufmg.br (F.M. Ribeiro).

https://doi.org/10.1016/j.neuint.2019.03.020
Received 22 January 2019; Received in revised form 20 March 2019; Accepted 26 March 2019
Available online 29 March 2019
0197-0186/ © 2019 Elsevier Ltd. All rights reserved.

abnormalities in microglial population (Davis et al., 1999; Streit et al., 2004). Moreover, it has been observed that aged-related inflammation can also contribute to neurodegenerative processes (von Bernhardi et al., 2015). Conversely, in the central nervous system (CNS), injury, aging or neurodegeneration can trigger inflammation, which is orchestrated by glial cells that, when stimulated, can become activated and release inflammatory mediators, changing their micro-environment (Wyss-Coray, 2016).

For decades, glutamate has been implicated in neurotoxicity, gaining prominence in studies concerning neurodegenerative processes (Choi, 1985, 1987; DiFiglia, 1990; Ribeiro et al., 2017). Glutamate acts through ionotropic and metabotropic glutamate receptors (mGlu receptors) (Willard and Koochekpour, 2013). The metabotropic glutamate receptor 5 ($mGlu_5$ receptor) is a $G\alpha q_{11}$-coupled receptor that belongs to Group I mGlu receptors. Stimulation of this receptor leads to activation of phospholipase Cβ1 (PLC), resulting in diacylglycerol and inositol-1,4,5-triphosphate (InsP3) formation and release of Ca^{2+} from intracellular stores (Abe et al., 1992). Diacylglycerol and Ca^{2+} then act together to trigger protein kinase C (PKC) activation, which can propagate signalization (Ribeiro et al., 2010; Willard and Koochekpour, 2013). In the brain of rodents, $mGlu_5$ receptor has already been shown to be mainly expressed in the olfactory bulb, striatum, lateral septum, cortex, nucleus accumbens and hippocampus (Romano et al., 1995; Shigemoto et al., 1993). $mGlu_5$ receptor is highly expressed in neurons, where it can modulate the postsynaptic response (Masu et al., 1991; Ribeiro et al., 2014; Volk et al., 2006; Willard and Koochekpour, 2013). Moreover, the receptor is also found in glial cells, including microglia and astrocytes (Biber et al., 1999; Byrnes et al., 2009).

$mGlu_5$ receptor has already been shown to play in important role in neuronal survival, although it is still a matter of debate whether receptor activation can rescue or exacerbate neuronal cell death (Abd-Elrahman et al., 2017; Doria et al., 2015; Rong et al., 2003). In terms of inflammation, pharmacological activation of $mGlu_5$ receptor was shown to prevent microglia activation and also microglia-induced neurotoxicity (Byrnes et al., 2009; Qiu et al., 2015; Xue et al., 2014; Zhang et al., 2015). Although the relevance of $mGlu_5$ receptor for neurodegenerative diseases and inflammation has been studied, its involvement in normal brain aging remains unclear.

To shed some light on this issue, we have employed $mGlu_5$ receptor knockout ($mGluR5^{-/-}$) mice at 2, 6 and 12 months of age and performed a series of histological and molecular studies. As a model of progressive neurodegeneration, we choose BACHD, a transgenic mouse model of Huntington's Disease (HD) that expresses mutant huntingtin (htt) containing 97 glutamines in the amino-terminal region (Gray et al., 2008). BACHD mice have a robust phenotype and exhibit age-dependent neurological decline (Doria et al., 2015; Gray et al., 2008). In addition, to determine whether the alterations triggered by $mGlu_5$ receptor ablation could be exacerbated by another insult, we employed double mutant mice ($mGluR5^{-/-}$/BACHD).

2. Methods

2.1. Material

Mouse anti-neuronal nuclei (NeuN) (Cat# MAB377, RRID: AB_2298772) and rat anti-CD68 (MCA, 1957) were from Bio-Rad. Rabbit anti-S100-β (Cat# ab52642) was from ABCAM and rabbit anti-ionized calcium binding adapter molecule 1 (IBA-1) (Cat# 019–19741) was from Wako chemicals. The goat anti-rat IgG (H + L) Cross-Adsorbed Secondary Antibody Alexa Fluor 546 (Cat# A11081), the goat anti-Rabbit IgG (H + L) Cross-Adsorbed Secondary Antibody, Alexa Fluor 488 (Cat# A-11008), TRIzol™ and Power SYBR™ Green PCR Master Mix, were purchased from Thermo Scientific. Vecta stain Elite ABC Kit (Mouse IgG and Rabbit IgG) and Vector SG Peroxidase Substrate Kit were purchased from Vector Laboratories (Burlingame, CA, USA). All other biochemical reagents were purchased from Sigma-Aldrich (St Louis, MO, USA).

2.2. Animals

FVB/NJ (wild-type, RRID: IMSR_JAX:001800) and FVB/N-Tg (HTT*97Q) IXwy/°J (BACHD) transgenic mice (Gray et al., 2008) and $mGlu_5$ receptor knockout B6; 129-$Grm5^{tm1Rod}$/J (*$mGluR5^{-/-}$*) mice (Lu et al., 1997) were purchased from The Jackson Laboratory (Bar Harbor, ME, USA). For the generation of the double mutants, $mGluR5^{-/-}$ mice and BACHD mice were crossed, obtaining the F1 parental lineage. Afterwards, F1 mice were crossed to obtain the lineages of interest (F2): WT, $mGluR5^{-/-}$, BACHD and BACHD/$mGluR5^{-/-}$ (double mutant). Only F1 mice were used for crosses and the heterozygous F2 mice were discarded. This study was conducted using littermate male mice at the ages of 2, 6 and 12 months. Mice were housed in an animal care facility at 23 °C on a 12 h light/12 h dark cycle with food and water provided ad libitum. All mice that were euthanized in this study were first anesthetized with ketamine/xylazine (80/8 mg/kg) i.p. before cervical dislocation. Animal care was in accordance with the Universidade Federal de Minas Gerais Ethics Committee on Animal Use, CEUA, 234/2016.

2.3. Immunohistochemistry

Brains from mice at 2, 6 and 12 months of age were dissected out and stored in 4% paraformaldehyde (PFA) in phosphate buffered saline (PBS) (137 mM NaCl, 2.7 mM KCl, 8 mM Na_2HPO_4, and 2 mM KH_2PO_4) for 72 h. Prior to sectioning, brains were put into 30% sucrose in PBS overnight at 4 °C. Brains were coronally sectioned in cryostat and 30 µm slices were stored in cryoprotect solution. Coronal slices containing both striatum and cortex were selected for immunohistochemistry analysis using a peroxidase-based immunostaining protocol to label free-floating sections. In brief, endogenous peroxidase activity was quenched using 0.3% hydrogen peroxide, washed 2 times per 5 min with 1 × PBS, after which the membranes were permeabilized using 1% Triton X-100 for 10 min. Non-specific binding was blocked for 30 min using 1.5% horse serum in the case of NeuN immunostaining or goat serum in the case of S100-β and IBA-1 immunostaining. Slices were incubated with either mouse anti-NeuN (1:100), rabbit anti-S100β (1:1000) or rabbit anti-IBA-1 (1:500) primary antibodies, in 2% normal horse or goat serum (from Vector Elite Kit) and 3% bovine serum albumin (BSA) in PBS overnight at 4 °C. Sections were washed in PBS and then incubated in secondary antibody, biotinylated horse anti-mouse (1:400, Vector Elite ABC kit mouse) or biotinylated goat anti-rabbit (1:400, Vector Elite ABC kit rabbit) for 90 min at 4 °C. Finally, sections were incubated in avidin–biotin enzyme reagent complex (from Vector Elite Kit) for 90 min at 4 °C, according to the manufacturer's instructions. Immunostaining was visualized using a chromogen (Vector SG substrate). Sections were mounted on slides and visualized using an Axio Imager A2-Carl Zeiss Microscope with a Zeiss 20 × lens, representative 710 µm × 532 µm areas of cortex or striatum were imaged for analyses. The number of NeuN, S100-β or IBA-1-positive puncta per image was counted by a blinded observer using the cell counter tool from ImageJ (NIH, USA, RRID:nif-0000-30467) as previously described (Doria et al., 2015).

2.4. Immunofluorescence and imaging

12-month-old mice were transcardially perfused with PBS and brains were dissected and stored in 4% PFA in PBS for 72 h and then infiltrated with 30% sucrose in PBS. Brains were coronally sectioned using a cryostat and 30 µm slices were stored in cryoprotect solution. Sections were washed 3 times for 30 min with TBST (TBS containing 0.5% Triton X-100). Slices were then incubated for 30 min in citrate buffer at 70 °C, washed 3 times of 10 min and blocked for 120 min using 4% BSA in TBST. Sections were incubated with rat anti-CD68 (1:1000)

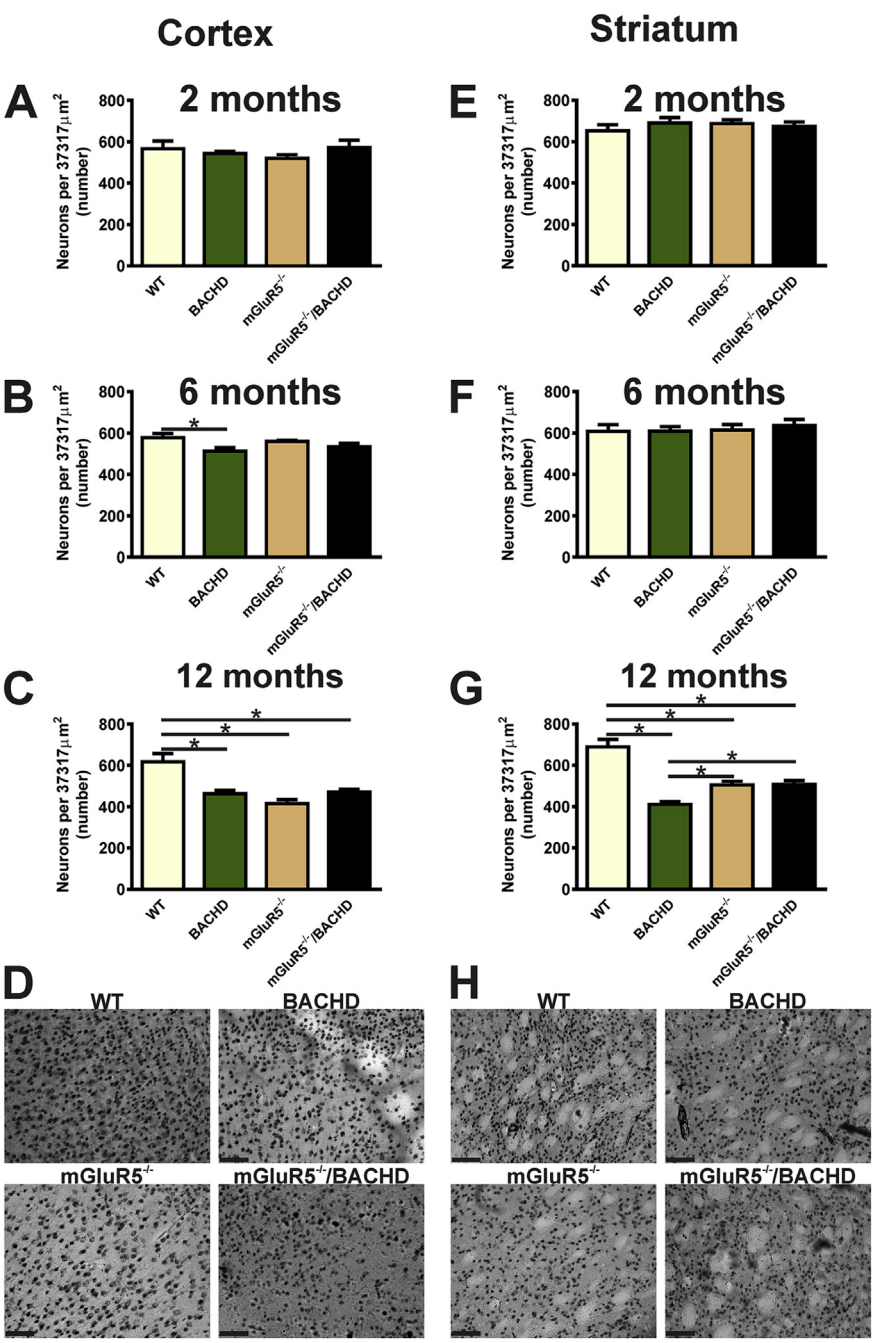

Fig. 1. Deletion of $mGlu_5$ receptor triggers neurodegeneration in the cortex and striatum of 12-month-old mice. Graphs show quantification of NeuN-labeled cortical (A, B and C) and striatal (E, F and G) neurons per 37,317 μm^2 in WT (n = 4), $mGluR5^{-/-}$ (n = 4), BACHD (n = 4) and BACHD/$mGluR5^{-/-}$ (n = 4) mice at 2 (A or E), 6 (B or F) and 12 months of age (C or G). Shown are representative images for NeuN immunostaining of the cortex (D) and striatum (H) from WT, $mGluR5^{-/-}$, BACHD and BACHD/$mGluR5^{-/-}$ mice at 12 months of age. Scale bar = 100 μm. Data represent the means ± SEM obtained from 6 images taken from 2 histological slices per mouse. * indicates significant difference as compared to WT or BACHD mice ($p < 0.05$).

and rabbit anti-IBA-1 (1:500) primary antibodies in blocking solution for 48 h at 4 °C. Sections were washed 3 times of 10 min in TBST and then incubated with rat anti-mouse antibody conjugated with Alexa Fluor 546 (1:1000) and goat anti-rabbit antibody conjugated with Alexa Fluor 488 (1:500) for 1 h at room temperature. Finally, brain sections were washed 6 times with TBST for 10 min each wash and mounted on slides to be imaged on a Zeiss LSM 880 confocal system. Image acquisition was performed using an EC Plan-Neofluar 40 × /1.30 Oil DIC M27 objective using the Zen 2 software. Image acquisition and analyses were performed as blind analyses by a different researcher who had not performed the immunofluorescence. Three images were collected for each slice, 2 slices were imaged per animal and experimental groups contained 6 animals each, totalizing 36 images for each experimental condition. Image files were acquired as z-stacks of 7 planes separated by 2.07 μm for imaging of multiple microglia in the same region. Stacks were processed for maximum intensity projection and subjected to pixel gray levels analyses. Mean pixel intensity was measured for the anti-CD68 signal per image (Fig. 4E) and normalized by the total number of IBA-1 positive cells (Fig. 4F). Image J software was used for all image analyses and processing.

2.5. Analyses of skeleton images

Microglia morphology analysis was performed by a skeleton analysis method according to Morrison and Filosa (2013) using the immunofluorescence confocal images obtained as described above. For skeleton analysis, the maximum intensity projection of the anti-IBA-1 signal was enhanced to visualize all microglia processes followed by noise de-speckling to eliminate single-pixel background fluorescence. The resulting image was converted to a binary image and then skeletonized using Image J software (Fig. 5). AnalyzeSkeleton plugin (https://imagej.net/AnalyzeSkeleton) was then used to process all

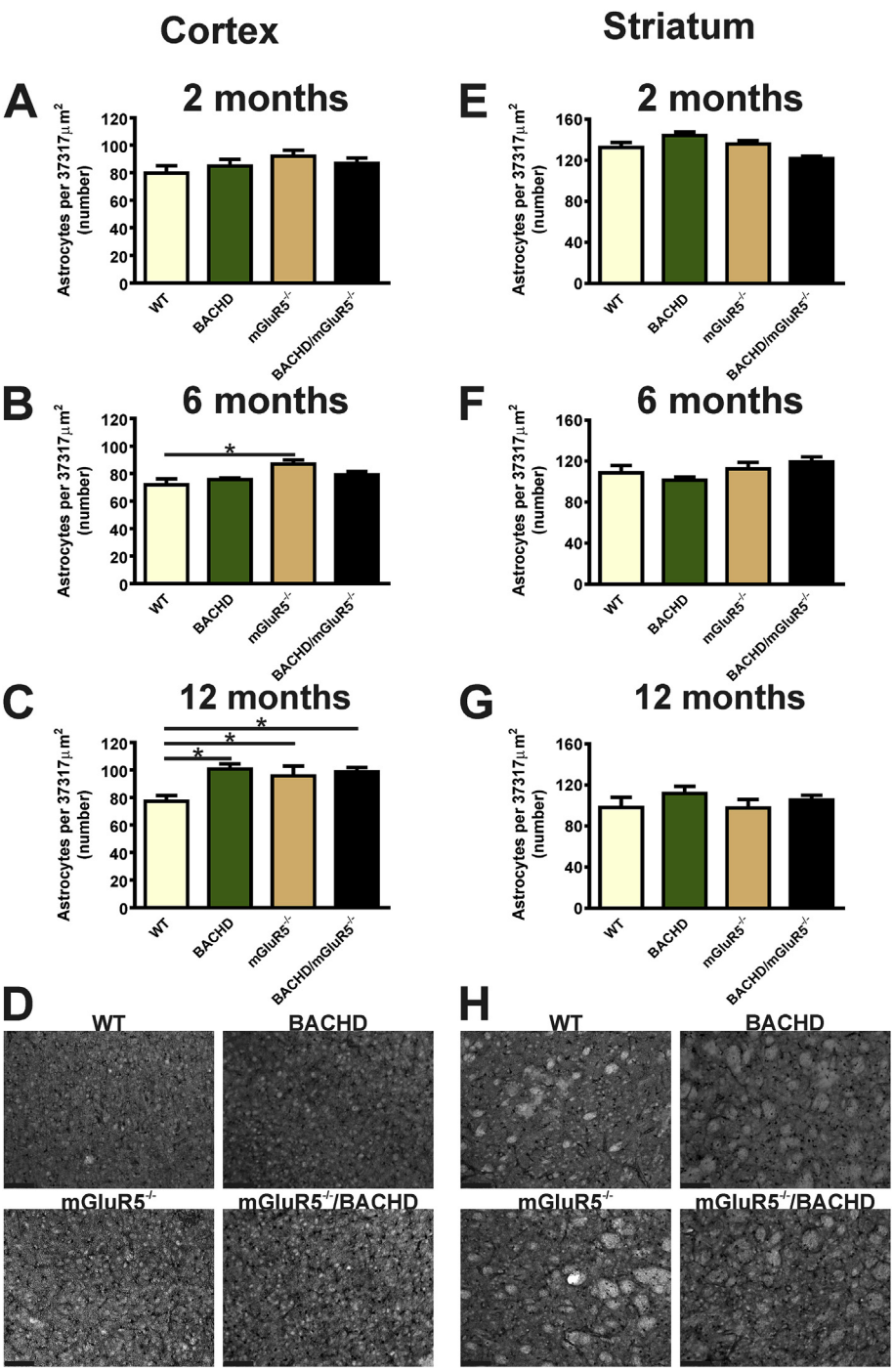

Fig. 2. mGluR5$^{-/-}$ showed astrogliosis in the cortical region at 6 and 12 months of age. Graphs show quantification of S100-β-labeled cortical (A, B and C) and striatal (E, F and G) astrocytes per 37,317 μm^2 in WT (n = 4), mGluR5$^{-/-}$ (n = 4), BACHD (n = 4) and BACHD/mGluR5$^{-/-}$ (n = 4) mice at 2 (A or E), 6 (B or F) and 12 months of age (C or G). Shown are representative images for S100-β immunostaining of the cortex (D) and striatum (H) from WT, mGluR5$^{-/-}$, BACHD and BACHD/mGluR5$^{-/-}$ mice at 12 months of age. Scale bar = 100 μm. Data represent the means ± SEM obtained from 6 images taken from 2 histological slices per mouse. * indicates significant difference as compared to WT mice ($p < 0.05$).

skeletonized images for data collection on the number of endpoints per microglia (Fig. 5, blue points), maximum length of branches (Fig. 5, orange slabs) and number of branches (Fig. 5, blue points, orange slabs and purple junction). The analyses were based on studies showing that there are morphological changes when microglia become activated (von Bernhardi et al., 2015). All microglia that were completely inside the field were selected for image analyses, resulting in a total of 36 cells analyzed per group.

2.6. Quantitative RT-qPCR

RNA from cortical samples of mice with 2, 6 and 12 months of age was isolated using TRIzol™ reagent as per manufacturer's instructions (Thermo Scientific). RNA was resuspended in 11 μL of nuclease-free water, and its concentration was analyzed by spectrophotometer (NanoDrop™, Thermo Scientific). cDNAs were prepared from 2 μg of total RNA extracted in a 20 μL final reverse transcription reaction. RT-qPCR was performed from 10 × diluted cDNA and using Power SYBR™ Green PCR Master Mix in the QuantStudio™ 7 Flex real-time PCR system platform (Applied Biosystems). RT-qPCR assays were performed to quantify mRNA levels of the following mus musculus genes: tumor necrosis factor (TNF-α); interleukin 1 beta (IL-1β); fractalkine (CX3CL1); CX3CR1; mus musculus MCP-1 and transforming growth factor-β 3 (TGF-β3). Primers were designed using Primer3Plus Program (26): TNF-α (forward: 5′-GCTGAGCTCAAACCCTGGTA-3′; reverse: 5′-CGGACTCCGCAAAGTCTAAG-3′); Il-1-β (forward: 5′-GGGCCTCAAA GGAAAGAATC-3′; reverse: 5′-TACCAGTTGGGGAACTCTGC-3′); CX3CL1 (forward: 5′- CGACAAGATGACCTCACGAA-3’; reverse: 5′-

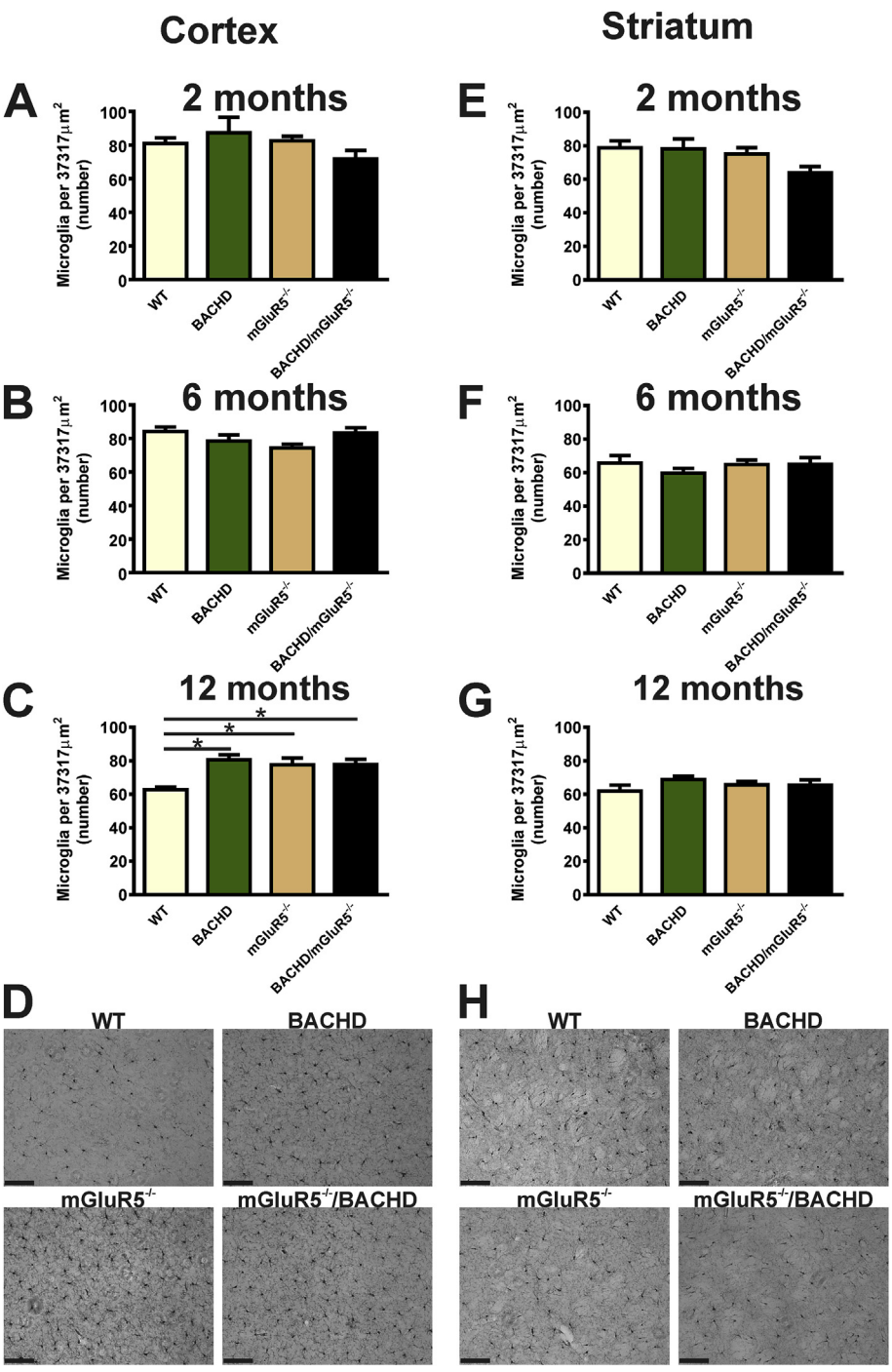

Fig. 3. Microgliosis is observed in the cortex of mGluR5$^{-/-}$ at 12 months of age. Graphs show quantification of IBA-1-labeled cortical (A, B and C) and striatal (E, F and G) microglia per 37,317 μm^2 in WT (n = 4), mGluR5$^{-/-}$ (n = 4), BACHD (n = 4) and BACHD/mGluR5$^{-/-}$ (n = 4) mice at 2 (A or E), 6 (B or F) and 12 months of age (C or G). Shown are representative images for IBA-1 immunostaining of the cortex (D) and striatum (H) from WT, mGluR5$^{-/-}$, BACHD and BACHD/mGluR5$^{-/-}$ mice at 12 months of age. Scale bar = 100 μm. Data represent the means ± SEM obtained from 6 images taken from 2 histological slices per mouse. * indicates significant difference as compared to WT mice ($p < 0.05$).

CTGTGTCGTCTCCAGGACAA-3′); CX3CR1 (forward: 5′-TGCCTTCTTC CTCTTCTGGA-3’; reverse: 5’ – TAAAGGGGTTGAGGCAACAG-3′); MCP-1 (forward: 5′-CCCAATGAGTAGGCTGGAGA-3’; reverse: 5′- GCTGAAG ACCTTAGGGCAGA-3); TGF-β3 (forward: 5′- TCTGCCCCAAAGGAATT ACC-3’; reverse: 5′- CTCCATTGGGCTGAAAGGTG-3′); actin (forward: 5′- AATGCCTGGGTACATGGTGGTA-3’; reverse: 5′- TGGAATCCTGTGG CATCCATGA-3′).

Previous verification of undesired secondary formations or dimers between primers were performed using “OligoAnalyser 3.1” tool (Integrated DNA Technologies©), available at https://www.idtdna.com/calc/analyzer. All primers used in this work were validated by serial dilution assay and the reaction efficiency was calculated, comprising 90–110% (data not shown). All RT-qPCRs showed good quality of amplification and changes in gene expression were determined with the $2^{-\Delta Ct}$ method using actin for normalization.

2.7. Statistical analyses

Means ± SEM are shown for the number of independent experiments indicated in Figure Legends. GraphPad Prism™ software was used to analyze data for statistical significance. Statistical significance ($p < 0.05$) was determined by analysis of variance (ANOVA) testing followed by Dunnett's multiple comparisons test and Tukey's multiple comparisons test, as indicated in each Figure Legend.

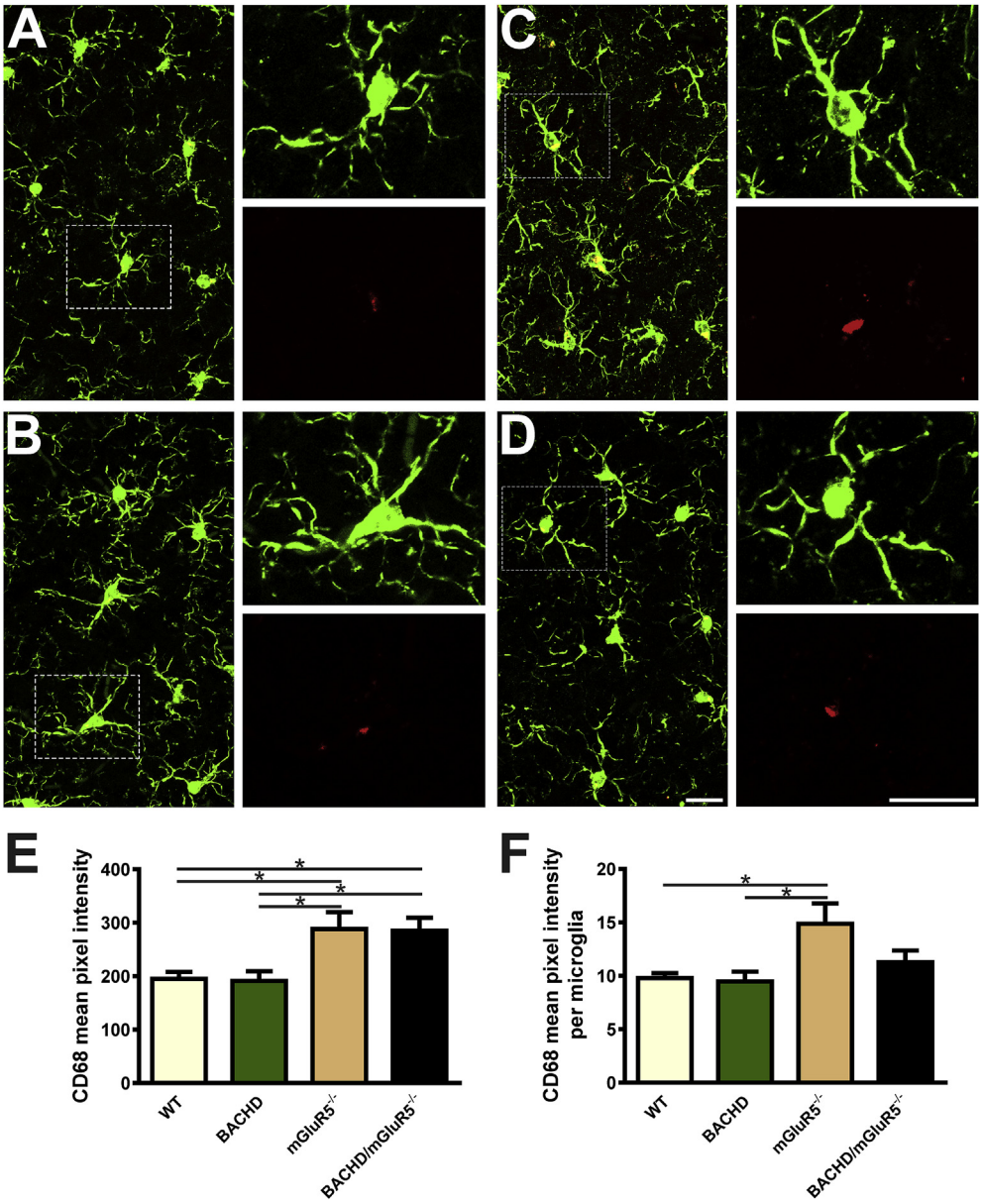

Fig. 4. Deletion of $mGlu_5$ receptor leads to microglia activation in the cortex of 12-month-old mice. Shown are representative laser scanning confocal micrographs of cortical slices from WT (A, n = 6), BACHD (B, n = 6), $mGluR5^{-/-}$ (C, n = 6) and BACHD/$mGluR5^{-/-}$ (D, n = 6) mice at 12 months of age. Immunofluorescence labeling was performed using anti-IBA-1 (green) and anti-CD-68 (red). Scale bar = 10 μm. Graphs show CD-68 mean pixel intensity per image (E) or CD-68 mean pixel intensity normalized by the number of microglia (F). Data represent the means ± SEM obtained from 6 images taken from 2 histological slices per mouse. * indicates significant difference ($p < 0.05$). (For interpretation of the references to colour in this figure legend, the reader is referred to the Web version of this article.)

3. Results

3.1. Ablation of $mGlu_5$ receptor evokes neuronal cell death in aged mice

It is well known that $mGlu_5$ receptor plays an important role in neuronal survival/neurodegeneration (Mao et al., 2005; Ribeiro et al., 2014; Rong et al., 2003). However, little is known about the role of $mGlu_5$ receptor in aging. Thus, we decided to investigate whether $mGluR5^{-/-}$ mice could exhibit altered levels of neuronal cell loss in an age-dependent manner. Therefore, we assessed cortical and striatal slices from $mGluR5^{-/-}$ and controls mice (WT) at 2, 6 and 12 months of age using an antibody to label a neuronal specific marker, NeuN. As a positive control, we employed the BACHD mice, a transgenic mouse model of Huntington's disease that has a progressive neurodegenerative phenotype (Gray et al., 2008), as well as double mutant mice (BACHD/$mGluR5^{-/-}$), which express mutant huntingtin protein in the absence of $mGlu_5$ receptor expression. At 2 months of age, there was no difference in the number of neurons when comparing the four groups of mice, regardless of whether striatum or cortex was analyzed (Fig. 1A and E). At 6 months of age, BACHD mice showed decreased neuronal population in the cortex (Fig. 1B), although no difference was observed in the case of the striatum (Fig. 1F). Finally, at 12 months of age, $mGluR5^{-/-}$ mice exhibited diminished number of neurons in both cortex and striatum, when compared to WT mice (Fig. 1C, D, 1G and 1H). Moreover, both BACHD and BACHD/$mGluR5^{-/-}$ mice at 12 months of age also exhibited decreased number of neurons, as compared to WT mice (Fig. 1C, D, 1G and 1H). Interestingly, the double mutant mice did not exhibit a more prominent decrease in the number of neurons, indicating that the knockout of $mGlu_5$ receptor and the expression of mutant htt do not appear to have an additive effect regarding neurodegeneration (Fig. 1C, D, 1G and 1H). In fact, $mGlu_5$ receptor ablation in BACHD mice appear to partially rescue the neurodegeneration induced by mutant htt in the striatum, as BACHD/$mGluR5^{-/-}$ mice exhibited increased number of neurons as compared to that of BACHD mice (Fig. 1G and H). These data highlight the dual role of $mGlu_5$ receptor in neuronal cell death processes. Moreover, these results also indicate that, similarly to the neurodegenerative mouse model, BACHD, $mGluR5^{-/-}$ mice exhibit age-related neurodegeneration in the cortex and striatum.

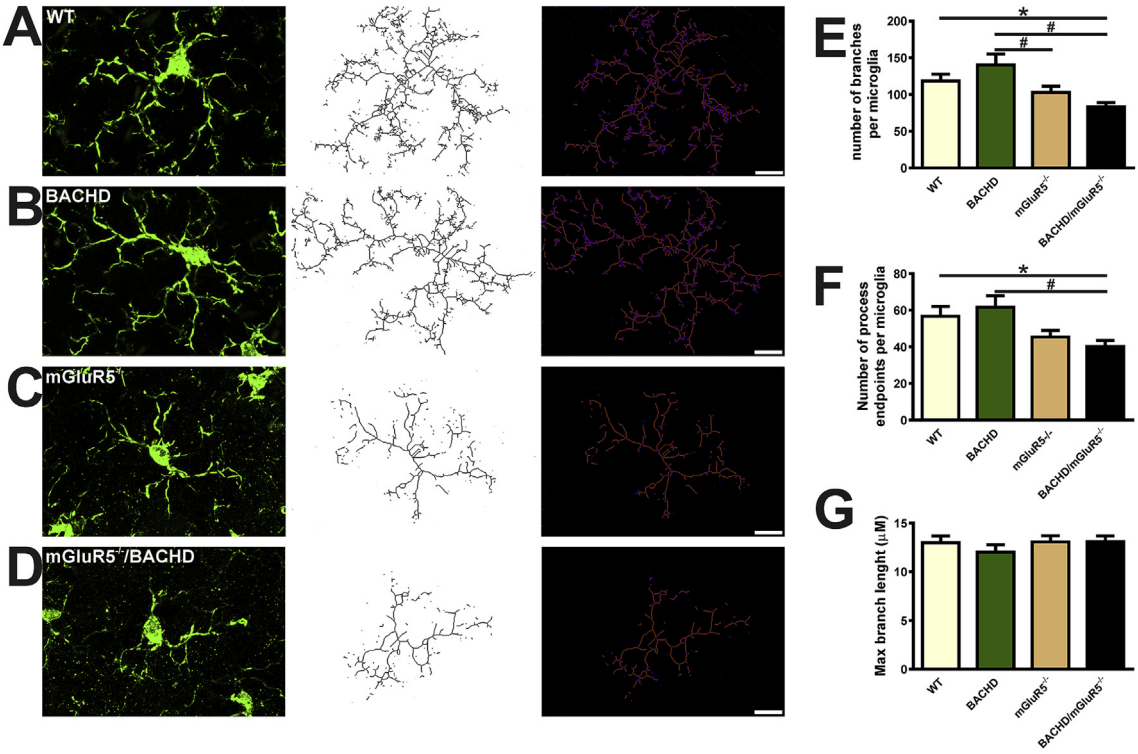

Fig. 5. Deletion of $mGlu_5$ receptor triggers morphological changes in the cortical region of 12-month-old mice. Shown are representative images for IBA-1 positive microglia from cortical slices, as well as their skeletonized and analyzed version, obtained from WT (A, n = 6), $mGluR5^{-/-}$ (B, n = 6), BACHD (C, n = 6) and BACHD/$mGluR5^{-/-}$ (D, n = 6) mice at 12 months of age. Scale bar = 10 μm. Graphs show the number of branches per microglia (the sum of blue points, orange slabs and purple junction) (E), the number of end points per microglia (blue points) (F) and the maximum length of branches (orange slabs) (G). * indicates significant difference as compared to WT ($p < 0.05$) and # indicates significant difference as compared to BACHD mice ($p < 0.05$). (For interpretation of the references to colour in this figure legend, the reader is referred to the Web version of this article.)

3.2. $mGluR5^{-/-}$ mice exhibit age-dependent gliosis

$mGlu_5$ receptor is not exclusively expressed by neurons, as it is also present in glial cells, including astrocytes and microglia, which are crucial cells for brain homeostasis but also for neuroinflammation (Biber et al., 1999; Byrnes et al., 2009). During neuroinflammation, which can be triggered not only by neurodegeneration but also by normal aging, glial cells can multiply and became activated (Aguzzi et al., 2013; Davies et al., 2017). Therefore, we decided to investigate whether the number of glial cells could be altered due to $mGlu_5$ receptor ablation. Astrocytes are the most abundant glial cell in the brain (Chung et al., 2015). Thus, we performed immunohistochemistry experiments using anti-S100-β antibody, which specifically labels astrocytes. Curiously, unlike what was observed in terms of neuronal cell loss (Fig. 1), the number of astrocytes was different in the cortex, but not in the striatum (Fig. 2). At 2 months of age, no difference was observed among the groups (Fig. 2A). However, at 6 months of age, $mGluR5^{-/-}$ mice already showed increased number of astrocytes as compared to WT mice (Fig. 2B). Moreover, at 12 months of age, $mGluR5^{-/-}$, BACHD and BACHD/$mGluR5^{-/-}$ mice exhibited astrogliosis, as compared to WT mice, but exclusively in the cortical region (Fig. 2C and D). Again, no additive effect was observed for mutant htt and $mGlu_5$ receptor knockout mice (Fig. 2C and D). Therefore, these results indicate that $mGlu_5$ receptor ablation promotes astrogliosis in an age-dependent manner and that the $mGluR5^{-/-}$ effect on the number of astrocytes occurs earlier than that triggered by mutant htt.

Microglial cells are the resident macrophages in the central nervous system and have an important role in aging, neurodegeneration and inflammation (Ransohoff and Perry, 2009; von Bernhardi et al., 2015; Wu et al., 2016; Wyss-Coray, 2016). To investigate whether the number of microglial cells is altered due to aging in $mGluR5^{-/-}$ mice, we performed immunohistochemistry experiments employing anti-IBA-1 to specifically label microglia. At 2 and 6 months of age, there was no significant difference in the number of microglial cells comparing the 4 groups of mice, regardless of whether striatal or cortical slices were analyzed (Fig. 3A, B, 3E and 3F). In addition, as previously seen in the case of astrocytes, the number of microglia was higher in the cortical region in $mGluR5^{-/-}$, BACHD and BACHD/$mGluR5^{-/-}$ mice at 12 months of age (Fig. 3C and D), although no changes were observed when striatal slices were investigated (Fig. 3G and H). Again, no additive effect for mutant htt and $mGlu_5$ receptor ablation was observed. Thus, these results show that knocking out $mGlu_5$ receptor or expressing mutant htt produces the same effect in terms of microgliosis.

3.3. $mGlu_5$ receptor knockout triggers microglia activation in elder mice

Because $mGluR5^{-/-}$, BACHD and BACHD/$mGluR5^{-/-}$ mice exhibited increased number of microglia in the cortex at 12 months of age, we decided to verify whether these microglia were activated. Microglia activation is a consistent finding that has been seen in brain undergoing normal aging, as well as in the brain of patients suffering from neurodegenerative diseases (Conde and Streit, 2006; Davies et al., 2017; von Bernhardi et al., 2015). Here, we immunostained cortical slices from 12-month-old mice using an anti-CD-68 antibody, which is employed as a microglia/macrophage activation marker (Vasek et al., 2016). Representative confocal images are shown in Fig. 4A, B, 4C and 4D. Interestingly, the sum of CD68 mean pixel intensity per image was increased in both $mGluR5^{-/-}$ and BACHD/$mGluR5^{-/-}$, as compared to WT and BACHD mice (Fig. 4E). Moreover, when CD68 mean pixel intensity per image was normalized by the number of microglia (IBA-1 positive cells), $mGluR5^{-/-}$ mice exhibited increased levels, as compared to that of either WT or BACHD mice (Fig. 4F).

It is already known that microglia obtained from young mice have a small cell body and long ramifications. However, due to aging, microglia tends to switch to an activated state, gradually showing bigger cell bodies and shorter cell processes (von Bernhardi et al., 2015). To perform morphological analysis, we employed cortical slices obtained from 12-month-old mice, which were labeled with anti-IBA-1 antibody. IBA-1 labeling was converted to a binary image and then skeletonized. Representative microglia images of all four genotypes with their respective skeletonized and analyzed images are shown in Fig. 5A, B, 5C and 5D. The number of branches per cell was significantly lower in mGluR5$^{-/-}$ when compared to BACHD mice (Fig. 5E). Notably, BACHD/mGluR5$^{-/-}$ exhibited reduced number of branches when compared to both WT and BACHD mice (Fig. 5E). Moreover, the number of process endpoints per cell was significantly decreased in BACHD/mGluR5$^{-/-}$ mice when compared to both WT and BACHD mice (Fig. 5F). When we assessed the maximum length of branches, we did not observe any difference among the groups (Fig. 5G). Together, these results clearly indicate that although mutant htt triggers microgliosis, it does not promote microglia activation. Ablation of mGlu$_5$ receptor, on the other hand, promotes both microgliosis and microglia activation in an age-dependent manner.

3.4. Presence of mutant htt and ablation of mGlu$_5$ receptor promote decreased levels of fractalkine expression in aged mice

Microglia activation is followed by increased expression of different cytokines and chemokines (von Bernhardi et al., 2015; von Bernhardi et al., 2010). Surprisingly, when we analyzed the levels of interleukin-1 β (IL1-β) (Sup. Fig. 1A), tumor necrosis factor-α (TNF-α) (Sup. Fig. 1B), transforming growth factor-β 3 (TGF-β3) (Sup. Fig. 1C) and monocyte chemoattractant protein 1 (MCP-1) (Sup. Fig. 1D) in cortical samples, we did not observe any difference comparing the four groups of mice. Then, we decided to assess fractalkine (CX3CL1), a chemokine that is produced by neurons and astrocytes and act on microglia, which are the only cells expressing the CX3CL1 receptor (CX3CR1) in the healthy brain (Pan et al., 1997; Paolicelli et al., 2014). We did not observe statistically significant changes in CX3CL1 expression levels when comparing the four groups of mice at 2 (Fig. 6A) and 6 (Fig. 6B) months of age. mGlu$_5$ receptor knockout appears to decrease the levels of CX3CL1 at 12 months of age, as compared to WT mice, although, this difference was not statistically significant (Fig. 6C). However, mutant htt and the absence of mGlu$_5$ receptor had a significant cumulative effect, decreasing the expression of CX3CL1 in the cortex of BACHD/mGluR5$^{-/-}$ mice at 12 months of age (Fig. 6C). The same effect was not observed in the case of CX3CR1 (Sup. Fig. 2). As CX3CL1 is important to regulate microglia activation, these results could, at least partially, explain the observed increased levels of microglia activation.

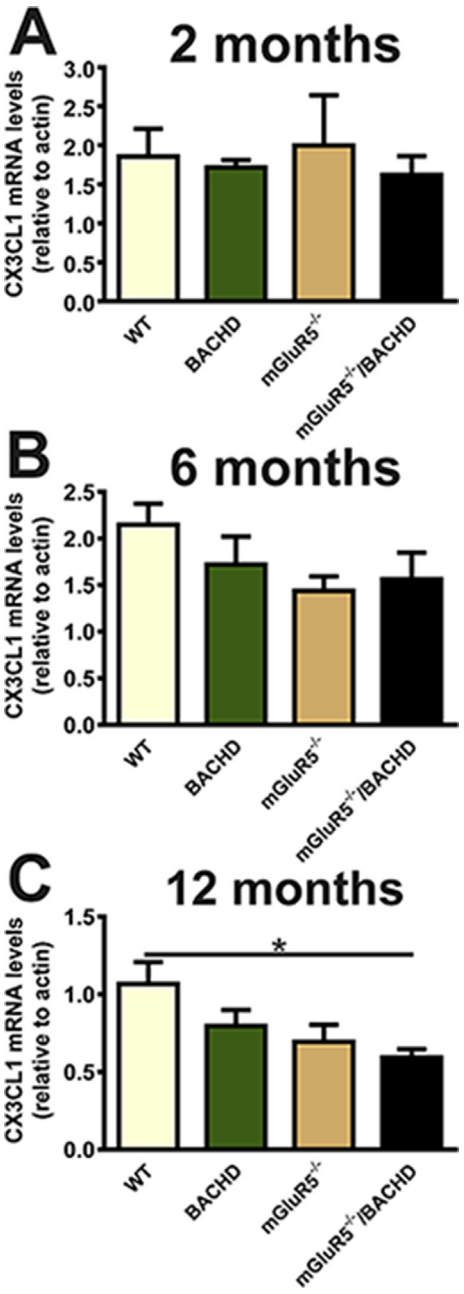

Fig. 6. Presence of mutant htt and ablation of mGlu$_5$ receptor promote decreased levels of fractalkine expression in 12-month-old mice. Graphs show mRNA levels of CX3CL1 in cortical samples from WT, mGluR5$^{-/-}$, BACHD, and BACHD/mGluR5$^{-/-}$ mice at 2 (A), 6 (B) and 12 months of age (C). mRNA levels were assessed by quantitative RT-PCR, which was performed in triplicate and normalized to actin mRNA levels. Data represent the means ± SEM, n = 6. * indicates significant difference ($p < 0.05$).

4. Discussion

Several alterations associated with normal brain aging have been reported as loss in gray matter density, cortical atrophy and dystrophic microglia, which were observed in normal subjects, as well as in mouse models of aging (Salat et al., 2004; Shimada, 1999; Sowell et al., 2003; Streit et al., 2004). In the present study, we demonstrated that mGluR5$^{-/-}$ mice exhibit neurodegeneration and neuroinflammation at 12 months of age, similarly to BACHD and mGluR5$^{-/-}$/BACHD mice. Thus, although mGlu$_5$ receptor was shown to be important in early brain development and in basic cellular processes such as proliferation and/or differentiation (Di Giorgi Gerevini et al., 2004), our data demonstrate that ablation of mGlu$_5$ receptor affects the number of neurons and glial cells in aged, but not in young mice.

We did not observe an additive effect for mutant htt and mGlu$_5$ receptor deletion in most results we obtained. A cumulative effect should be expected, as mutant htt and mGlu$_5$ receptor probably influence distinct pathways to promote their effect. However, it has been shown that mGlu$_5$ receptor and mutant htt share cell signalling pathways that are important for regulating gene expression. For instance, mGlu$_5$ receptor stimulation leads to cAMP responsive element binding protein (CREB) activation (Mao and Wang, 2003). Moreover, mutant htt also modulates CREB by sequestering its co-activator, CREB binding protein (CBP), inhibiting CREB-mediated gene transcription (Nucifora et al., 2001). Therefore, mGlu$_5$ receptor ablation and mutant htt expression have the same negative effect on CREB. It is well known that CREB is important for the expression of genes that are crucial for neuronal survival, including the brain derived neurotrophic factor (BDNF) (Giampa et al., 2013; Jeong et al., 2011; Panja and Bramham,

2014). Moreover, it has been proposed that CREB can modulate inflammatory responses (Wen et al., 2010). For instance, it has been proposed that CREB could inhibit NF-kB activity (Brautigam et al., 2005). Therefore, the lack of additive effect for $mGlu_5$ receptor ablation and mutant htt could be explained by the fact that these two insults could be acting on the same cell signalling pathways. Future studies will be important to clarify this matter.

It is well known that neurodegeneration can trigger neuroinflammation (Ransohoff, 2016). Therefore, the gliosis and microglia activation observed in this study could be explained by the neuronal cell loss that was detected in the tested mouse models. However, we observed neuronal cell loss in both the cortex and striatum, although gliosis was exclusively observed in the cortex. In addition, $mGluR5^{-/-}$ mice already showed increased number of astrocytes, but no neurodegeneration, at 6 months of age in the cortical region, whereas 6-month-old BACHD mice exhibited neuronal cell loss in the cortex, without any obvious glial proliferation. Therefore, these results suggest that factors other than neurodegeneration could be contributing to cortical gliosis. It is unclear what factors could favor gliosis in the cortex, but not in the striatum. However, it is becoming more clear by recent studies that glial cells differ according to brain region. For instance, a recent study showed that astrocytes change their gene expression profiles across mouse lifespan in a regionally specific manner (Clarke et al., 2018). In addition, microglia localization in the brain also influences their genome expression profile in an age-dependent manner (Grabert et al., 2016). It is well known that $mGlu_5$ receptor can regulate gene transcription (Gass and Olive, 2008) and that the receptor activates different cell effectors and has different roles depending on whether cortex or striatum is being analyzed (Gandhi et al., 2008; Ribeiro et al., 2009). Thus, we hypothesize that the deletion of $mGlu_5$ receptor in the cortex, but not in the striatum, may lead to changes in astrocyte/microglia gene expression, which could account for the gliosis and microglia activation observed in the cortical region.

In the present study, although BACHD mice exhibited high levels of glial proliferation in the cortex, microglia activation was not observed. Although microglia activation has already been demonstrated in brains of patients with HD, this event is still controversial in murine models of HD (Mantovani et al., 2016; Simmons et al., 2016; Tai et al., 2007a, b). For instance, microglia proliferation was reported in BACHD mice previously (Simmons et al., 2016), although no microglia activation has been observed (Petkau et al., 2019). Moreover, it is possible that if BACHD mice were analyzed at a later age, it would exhibit microglia activation. Unexpectedly, when CD68 expression and microglia morphology were analyzed, deletion of $mGlu_5$ receptor was efficient to trigger microglia activation. Accordingly, Byrnes et al. (2009) demonstrated that acute treatment with $mGlu_5$ receptor agonist inhibits microglia activation in cell culture through the PLC/PKC pathway. Thus, surprisingly, $mGlu_5$ receptor ablation appears to be more deleterious in terms of neuroinflammation than mutant htt.

The results shown here indicated no changes in the expression levels of cytokines, when either mutant htt was present or $mGlu_5$ receptor was ablated. However, the presence of both mutant htt and $mGlu_5$ receptor deletion promoted decreased levels of CX3CL1 expression in aged mice. Microglia, both in healthy aging and during neurodegenerative diseases, are negatively or positively regulated mainly by neurons, but also by astrocytes (Ransohoff and Cardona, 2010). The CX3CL1-CX3CR1 axis constitutes one of the mechanisms to contain exacerbated microglia responses, in an attempt to maintain homeostasis in the CNS (Paolicelli et al., 2014). Consistent with this idea is the fact that microglia activation is the result of not only the action of activation mediators, but also the absence of inhibition. The relevance of CX3CL1-CX3CR1 regulation in the activation of microglia *in vivo* was demonstrated by Cardona et al. (2006). After peripheral injections of LPS, the $CX3CR1^{-/-}$ mice showed greater microglia activation and neurotoxicity. In a model of Parkinson's Disease and in a transgenic mouse model of amyotrophic lateral sclerosis, the $CX3CR1^{-/-}$ group showed more neuronal cell loss than control and intense inflammatory processes (Cardona et al., 2006). Therefore, these data corroborate our hypothesis that the decrease in CX3CL1 expression seen mainly in BACHD/$mGluR5^{-/-}$ mice may contribute to microglia activation in these animals. Future studies will be important to establish this relationship and to uncover other factors that could be important for microglia activation in $mGluR5^{-/-}$ mice, as, although CX3CL1 was slighted augmented in these animals, this difference did not reach statistical significance.

5. Conclusion

Our data clearly show that $mGluR5^{-/-}$ mice is a more robust model of aging than BACHD mice, even though the latter is considered an HD mouse model with a very intense phenotype (Menalled et al., 2009). In terms of neurodegeneration, knocking out $mGlu_5$ receptor was as deleterious as expressing mutant htt, whereas, regarding neuroinflammation, $mGlu_5$ receptor ablation was more harmful than HD. These results raise new implications for the use of $mGlu_5$ receptor blockers as drugs to treat neurological disorders. $mGlu_5$ receptor antagonists have been proposed to treat Alzheimer's disease (Abd-Elrahman et al., 2018; Hamilton et al., 2016), fragile x syndrome (Michalon et al., 2012), among others. Caution should be taken, especially if $mGlu_5$ receptor blockers are proposed to be used to treat chronic diseases, which will demand long term treatment, as this could prone patients to neuroinflammation. This study also highlights the importance of studying the role of $mGlu_5$ receptor in normal aging to further understand the role of this receptor in the brain. Although $mGlu_5$ receptor was ablated since the beginning of mouse life, which could implicate in developmental alterations that would not be observed when a receptor blocker is used, most of the alterations were observed in older mice, indicating that $mGlu_5$ receptor blockade during aging could reflect in serious deleterious results to the brain.

Declarations of interest

None.

Funding sources

This work was supported by CNPq [grant number 429049/2018-8] and FAPEMIG [grant number PPM-00212-18] grants to F. M. R.

Acknowledgements

The authors would like to thank the Center for Acquisition and Processing of Images (CAPI/ICB/UFMG) for providing the equipment for experiments involving confocal images.

Appendix A. Supplementary data

Supplementary data to this article can be found online at https://doi.org/10.1016/j.neuint.2019.03.020.

References

Abd-Elrahman, K.S., Hamilton, A., Hutchinson, S.R., Liu, F., Russell, R.C., Ferguson, S.S.G., 2017. mGluR5 antagonism increases autophagy and prevents disease progression in the zQ175 mouse model of Huntington's disease. Sci. Signal. 10.

Abd-Elrahman, K.S., Hamilton, A., Vasefi, M., Ferguson, S.S.G., 2018. Autophagy is increased following either pharmacological or genetic silencing of mGluR5 signaling in Alzheimer's disease mouse models. Mol. Brain 11, 19.

Abe, T., Sugihara, H., Nawa, H., Shigemoto, R., Mizuno, N., Nakanishi, S., 1992. Molecular characterization of a novel metabotropic glutamate receptor mGluR5 coupled to inositol phosphate/Ca2+ signal transduction. J. Biol. Chem. 267, 13361–13368.

Aguzzi, A., Barres, B.A., Bennett, M.L., 2013. Microglia: scapegoat, saboteur, or something else? Science 339, 156–161.

Biber, K., Laurie, D.J., Berthele, A., Sommer, B., Tolle, T.R., Gebicke-Harter, P.J., van Calker, D., Boddeke, H.W., 1999. Expression and signaling of group I metabotropic

glutamate receptors in astrocytes and microglia. J. Neurochem. 72, 1671–1680.
Brautigam, V.M., Frasier, C., Nikodemova, M., Watters, J.J., 2005. Purinergic receptor modulation of BV-2 microglial cell activity: potential involvement of p38 MAP kinase and CREB. J. Neuroimmunol. 166, 113–125.
Byrnes, K.R., Stoica, B., Loane, D.J., Riccio, A., Davis, M.I., Faden, A.I., 2009. Metabotropic glutamate receptor 5 activation inhibits microglial associated inflammation and neurotoxicity. Glia 57, 550–560.
Cardona, A.E., Pioro, E.P., Sasse, M.E., Kostenko, V., Cardona, S.M., Dijkstra, I.M., Huang, D., Kidd, G., Dombrowski, S., Dutta, R., Lee, J.C., Cook, D.N., Jung, S., Lira, S.A., Littman, D.R., Ransohoff, R.M., 2006. Control of microglial neurotoxicity by the fractalkine receptor. Nat. Neurosci. 9, 917–924.
Choi, D.W., 1985. Glutamate neurotoxicity in cortical cell culture is calcium dependent. Neurosci. Lett. 58, 293–297.
Choi, D.W., 1987. Ionic dependence of glutamate neurotoxicity. J. Neurosci. 7, 369–379.
Chung, W.S., Welsh, C.A., Barres, B.A., Stevens, B., 2015. Do glia drive synaptic and cognitive impairment in disease? Nat. Neurosci. 18, 1539–1545.
Clarke, L.E., Liddelow, S.A., Chakraborty, C., Munch, A.E., Heiman, M., Barres, B.A., 2018. Normal aging induces A1-like astrocyte reactivity. Proc. Natl. Acad. Sci. U. S. A. 115, E1896–E1905.
Conde, J.R., Streit, W.J., 2006. Microglia in the aging brain. J. Neuropathol. Exp. Neurol. 65, 199–203.
Davies, D.S., Ma, J., Jegathees, T., Goldsbury, C., 2017. Microglia show altered morphology and reduced arborization in human brain during aging and Alzheimer's disease. Brain Pathol. 27, 795–808.
Davis, D.G., Schmitt, F.A., Wekstein, D.R., Markesbery, W.R., 1999. Alzheimer neuropathologic alterations in aged cognitively normal subjects. J. Neuropathol. Exp. Neurol. 58, 376–388.
Di Giorgi Gerevini, V.D., Caruso, A., Cappuccio, I., Ricci Vitiani, L., Romeo, S., Della Rocca, C., Gradini, R., Melchiorri, D., Nicoletti, F., 2004. The mGlu5 metabotropic glutamate receptor is expressed in zones of active neurogenesis of the embryonic and postnatal brain. Brain Res Dev Brain Res 150, 17–22.
DiFiglia, M., 1990. Excitotoxic injury of the neostriatum: a model for Huntington's disease. Trends Neurosci. 13, 286–289.
Doria, J.G., de Souza, J.M., Andrade, J.N., Rodrigues, H.A., Guimaraes, I.M., Carvalho, T.G., Guatimosim, C., Dobransky, T., Ribeiro, F.M., 2015. The mGluR5 positive allosteric modulator, CDPPB, ameliorates pathology and phenotypic signs of a mouse model of Huntington's disease. Neurobiol. Dis. 73, 163–173.
Gandhi, R., Luk, K.C., Rymar, V.V., Sadikot, A.F., 2008. Group I mGluR5 metabotropic glutamate receptors regulate proliferation of neuronal progenitors in specific forebrain developmental domains. J. Neurochem. 104, 155–172.
Gass, J.T., Olive, M.F., 2008. Transcriptional profiling of the rat frontal cortex following administration of the mGlu5 receptor antagonists MPEP and MTEP. Eur. J. Pharmacol. 584, 253–262.
Giampa, C., Montagna, E., Dato, C., Melone, M.A., Bernardi, G., Fusco, F.R., 2013. Systemic delivery of recombinant brain derived neurotrophic factor (BDNF) in the R6/2 mouse model of Huntington's disease. PLoS One 8, e64037.
Grabert, K., Michoel, T., Karavolos, M.H., Clohisey, S., Baillie, J.K., Stevens, M.P., Freeman, T.C., Summers, K.M., McColl, B.W., 2016. Microglial brain region-dependent diversity and selective regional sensitivities to aging. Nat. Neurosci. 19, 504–516.
Gray, M., Shirasaki, D.I., Cepeda, C., Andre, V.M., Wilburn, B., Lu, X.H., Tao, J., Yamazaki, I., Li, S.H., Sun, Y.E., Li, X.J., Levine, M.S., Yang, X.W., 2008. Full-length human mutant huntingtin with a stable polyglutamine repeat can elicit progressive and selective neuropathogenesis in BACHD mice. J. Neurosci. 28, 6182–6195.
Hamilton, A., Vasefi, M., Vander Tuin, C., McQuaid, R.J., Anisman, H., Ferguson, S.S., 2016. Chronic pharmacological mGluR5 inhibition prevents cognitive impairment and reduces pathogenesis in an Alzheimer disease mouse model. Cell Rep. 15, 1859–1865.
Jeong, H., Cohen, D.E., Cui, L., Supinski, A., Savas, J.N., Mazzulli, J.R., Yates 3rd, J.R., Bordone, L., Guarente, L., Krainc, D., 2011. Sirt1 mediates neuroprotection from mutant huntingtin by activation of the TORC1 and CREB transcriptional pathway. Nat. Med. 18, 159–165.
Lu, Y.-M., Jia, Z., Janus, C., Henderson, J.T., Gerlai, R., Wojtowicz, J.M., Roder, J.C., 1997. Mice lacking metabotropic glutamate receptor 5 show impaired learning and reduced CA1 long-term potentiation (LTP) but normal CA3 LTP. J. Neurosci. 17, 5196–5205.
Mantovani, S., Gordon, R., Li, R., Christie, D.C., Kumar, V., Woodruff, T.M., 2016. Motor deficits associated with Huntington's disease occur in the absence of striatal degeneration in BACHD transgenic mice. Hum. Mol. Genet. 25, 1780–1791.
Mao, L., Wang, J.Q., 2003. Phosphorylation of cAMP response element-binding protein in cultured striatal neurons by metabotropic glutamate receptor subtype 5. J. Neurochem. 84, 233–243.
Mao, L., Yang, L., Tang, Q., Samdani, S., Zhang, G., Wang, J.Q., 2005. The scaffold protein Homer1b/c links metabotropic glutamate receptor 5 to extracellular signal-regulated protein kinase cascades in neurons. J. Neurosci. 25, 2741–2752.
Masu, M., Tanabe, Y., Tsuchida, K., Shigemoto, R., Nakanishi, S., 1991. Sequence and expression of a metabotropic glutamate receptor. Nature 349, 760–765.
Menalled, L., El-Khodor, B.F., Patry, M., Suarez-Farinas, M., Orenstein, S.J., Zahasky, B., Leahy, C., Wheeler, V., Yang, X.W., MacDonald, M., Morton, A.J., Bates, G., Leeds, J., Park, L., Howland, D., Signer, E., Tobin, A., Brunner, D., 2009. Systematic behavioral evaluation of Huntington's disease transgenic and knock-in mouse models. Neurobiol. Dis. 35, 319–336.
Michalon, A., Sidorov, M., Ballard, T.M., Ozmen, L., Spooren, W., Wettstein, J.G., Jaeschke, G., Bear, M.F., Lindemann, L., 2012. Chronic pharmacological mGlu5 inhibition corrects fragile X in adult mice. Neuron 74, 49–56.
Morrison, H.W., Filosa, J.A., 2013. A quantitative spatiotemporal analysis of microglia morphology during ischemic stroke and reperfusion. J. Neuroinflammation 10, 4.
Nucifora Jr., F.C., Sasaki, M., Peters, M.F., Huang, H., Cooper, J.K., Yamada, M., Takahashi, H., Tsuji, S., Troncoso, J., Dawson, V.L., Dawson, T.M., Ross, C.A., 2001. Interference by huntingtin and atrophin-1 with cbp-mediated transcription leading to cellular toxicity. Science 291, 2423–2428.
Pan, Y., Lloyd, C., Zhou, H., Dolich, S., Deeds, J., Gonzalo, J.A., Vath, J., Gosselin, M., Ma, J., Dussault, B., Woolf, E., Alperin, G., Culpepper, J., Gutierrez-Ramos, J.C., Gearing, D., 1997. Neurotactin, a membrane-anchored chemokine upregulated in brain inflammation. Nature 387, 611–617.
Panja, D., Bramham, C.R., 2014. BDNF mechanisms in late LTP formation: a synthesis and breakdown. Neuropharmacology 76 Pt C, 664–676.
Paolicelli, R.C., Bisht, K., Tremblay, M.E., 2014. Fractalkine regulation of microglial physiology and consequences on the brain and behavior. Front. Cell. Neurosci. 8, 129.
Petkau, T.L., Hill, A., Connolly, C., Lu, G., Wagner, P., Kosior, N., Blanco, J., Leavitt, B.R., 2019. Mutant huntingtin expression in microglia is neither required nor sufficient to cause the Huntington's disease-like phenotype in BACHD mice. Hum. Mol. Genet (Epub ahead of print).
Qiu, J.L., Zhu, W.L., Lu, Y.J., Bai, Z.F., Liu, Z.G., Zhao, P., Sun, C., Zhang, Y.B., Li, H., Liu, W., 2015. The selective mGluR5 agonist CHPG attenuates SO2-induced oxidative stress and inflammation through TSG-6/NF-kappaB pathway in BV2 microglial cells. Neurochem. Int. 85–86, 46–52.
Ransohoff, R.M., 2016. How neuroinflammation contributes to neurodegeneration. Science 353, 777–783.
Ransohoff, R.M., Cardona, A.E., 2010. The myeloid cells of the central nervous system parenchyma. Nature 468, 253–262.
Ransohoff, R.M., Perry, V.H., 2009. Microglial physiology: unique stimuli, specialized responses. Annu. Rev. Immunol. 27, 119–145.
Ribeiro, F.M., Ferreira, L.T., Paquet, M., Cregan, T., Ding, Q., Gros, R., Ferguson, S.S., 2009. Phosphorylation-independent regulation of metabotropic glutamate receptor 5 desensitization and internalization by G protein-coupled receptor kinase 2 in neurons. J. Biol. Chem. 284, 23444–23453.
Ribeiro, F.M., Hamilton, A., Doria, J.G., Guimaraes, I.M., Cregan, S.P., Ferguson, S.S., 2014. Metabotropic glutamate receptor 5 as a potential therapeutic target in Huntington's disease. Expert Opin. Ther. Targets 18, 1293–1304.
Ribeiro, F.M., Paquet, M., Cregan, S.P., Ferguson, S.S., 2010. Group I metabotropic glutamate receptor signalling and its implication in neurological disease. CNS Neurol. Disord. - Drug Targets 9, 574–595.
Ribeiro, F.M., Vieira, L.B., Pires, R.G., Olmo, R.P., Ferguson, S.S., 2017. Metabotropic glutamate receptors and neurodegenerative diseases. Pharmacol. Res. 115, 179–191.
Romano, C., Sesma, M.A., McDonald, C.T., O'Malley, K., Van den Pol, A.N., Olney, J.W., 1995. Distribution of metabotropic glutamate receptor mGluR5 immunoreactivity in rat brain. J. Comp. Neurol. 355, 455–469.
Rong, R., Ahn, J.Y., Huang, H., Nagata, E., Kalman, D., Kapp, J.A., Tu, J., Worley, P.F., Snyder, S.H., Ye, K., 2003. PI3 kinase enhancer-Homer complex couples mGluRI to PI3 kinase, preventing neuronal apoptosis. Nat. Neurosci. 6, 1153–1161.
Salat, D.H., Buckner, R.L., Snyder, A.Z., Greve, D.N., Desikan, R.S., Busa, E., Morris, J.C., Dale, A.M., Fischl, B., 2004. Thinning of the cerebral cortex in aging. Cerebr. Cortex 14, 721–730.
Shigemoto, R., Nomura, S., Ohishi, H., Sugihara, H., Nakanishi, S., Mizuno, N., 1993. Immunohistochemical localization of a metabotropic glutamate receptor, mGluR5, in the rat brain. Neurosci. Lett. 163, 53–57.
Shimada, A., 1999. Age-dependent cerebral atrophy and cognitive dysfunction in SAMP10 mice. Neurobiol. Aging 20, 125–136.
Simmons, D.A., Belichenko, N.P., Ford, E.C., Semaan, S., Monbureau, M., Aiyaswamy, S., Holman, C.M., Condon, C., Shamloo, M., Massa, S.M., Longo, F.M., 2016. A small molecule p75NTR ligand normalizes signalling and reduces Huntington's disease phenotypes in R6/2 and BACHD mice. Hum. Mol. Genet. 25, 4920–4938.
Sowell, E.R., Peterson, B.S., Thompson, P.M., Welcome, S.E., Henkenius, A.L., Toga, A.W., 2003. Mapping cortical change across the human life span. Nat. Neurosci. 6, 309–315.
Streit, W.J., Sammons, N.W., Kuhns, A.J., Sparks, D.L., 2004. Dystrophic microglia in the aging human brain. Glia 45, 208–212.
Tai, Y.F., Pavese, N., Gerhard, A., Tabrizi, S.J., Barker, R.A., Brooks, D.J., Piccini, P., 2007a. Imaging microglial activation in Huntington's disease. Brain Res. Bull. 72, 148–151.
Tai, Y.F., Pavese, N., Gerhard, A., Tabrizi, S.J., Barker, R.A., Brooks, D.J., Piccini, P., 2007b. Microglial activation in presymptomatic Huntington's disease gene carriers. Brain 130, 1759–1766.
United Nations, 2017. United Nations, Department of Economic and Social Affairs, Population Division (2017). World Population Ageing 2017 - Highlights (ST/ESA/SER.A/397).
Vasek, M.J., Garber, C., Dorsey, D., Durrant, D.M., Bollman, B., Soung, A., Yu, J., Perez-Torres, C., Frouin, A., Wilton, D.K., Funk, K., DeMasters, B.K., Jiang, X., Bowen, J.R., Mennerick, S., Robinson, J.K., Garbow, J.R., Tyler, K.L., Suthar, M.S., Schmidt, R.E., Stevens, B., Klein, R.S., 2016. A complement-microglial axis drives synapse loss during virus-induced memory impairment. Nature 534, 538–543.
Volk, L.J., Daly, C.A., Huber, K.M., 2006. Differential roles for group 1 mGluR subtypes in induction and expression of chemically induced hippocampal long-term depression. J. Neurophysiol. 95, 2427–2438.
von Bernhardi, R., Eugenin-von Bernhardi, L., Eugenin, J., 2015. Microglial cell dysregulation in brain aging and neurodegeneration. Front. Aging Neurosci. 7, 124.
von Bernhardi, R., Tichauer, J.E., Eugenin, J., 2010. Aging-dependent changes of microglial cells and their relevance for neurodegenerative disorders. J. Neurochem. 112, 1099–1114.
Wen, A.Y., Sakamoto, K.M., Miller, L.S., 2010. The role of the transcription factor CREB in

immune function. J. Immunol. 185, 6413–6419.
Willard, S.S., Koochekpour, S., 2013. Glutamate, glutamate receptors, and downstream signaling pathways. Int. J. Biol. Sci. 9, 948–959.
Wu, Z., Yu, J., Zhu, A., Nakanishi, H., 2016. Nutrients, microglia aging, and brain aging. Oxid Med Cell Longev 7498528 2016.
Wyss-Coray, T., 2016. Ageing, neurodegeneration and brain rejuvenation. Nature 539, 180–186.
Xue, F., Stoica, B.A., Hanscom, M., Kabadi, S.V., Faden, A.I., 2014. Positive allosteric modulators (PAMs) of metabotropic glutamate receptor 5 (mGluR5) attenuate microglial activation. CNS Neurol. Disord. - Drug Targets 13, 558–566.
Zhang, Z.Y., Sun, B.L., Liu, J.K., Yang, M.F., Li, D.W., Fang, J., Zhang, S., Yuan, Q.L., Huang, S.L., 2015. Activation of mGluR5 attenuates microglial activation and neuronal apoptosis in early brain injury after experimental subarachnoid hemorrhage in rats. Neurochem. Res. 40, 1121–1132.